AJNR

Angiographic CT in Cerebrovascular Stenting

Götz Benndorf, Charles M. Strother, Benjamin Claus, Ramin Naeini, Hesham Morsi, Richard Klucznik and Michael E. Mawad

AJNR Am J Neuroradiol 2005, 26 (7) 1813-1818
http://www.ajnr.org/content/26/7/1813

AJNR Am J Neuroradiol 26:1813–1818, August 2005

Technical Note

Angiographic CT in Cerebrovascular Stenting

Götz Benndorf, Charles M. Strother, Benjamin Claus, Ramin Naeini, Hesham Morsi, Richard Klucznik, and Michael E. Mawad

Summary: We evaluated the feasibility of angiographic CT (ACT) for visualizing metallic stents in three patients who underwent intracranial (n = 2) or extracranial (n = 1) stent placement to treat atherosclerotic lesions. ACT is a new technique that provides cross-sectional CT-like images based on rotational radiography performed with a rotating C-arm–mounted flat-panel detector. ACT allowed for the clear visualization of stents in both intracranial and extracranial arteries and was superior to conventional digital subtraction angiography and digital radiography in visualizing both the stent struts and their relationships to the arterial walls and aneurysmal lumen.

The use of intracranial stents has rapidly expanded over the past 5 years, particularly since the introduction of small, self-expandable stents developed specifically for the endovascular treatment of intracranial aneurysms. The small size and tortuous anatomy of intracranial arteries require that stents used in the intracranial vasculature have a low profile, high flexibility, and excellent trackability. Providing these features limits the degree of radiopacity that can be incorporated into the stents, Therefore, intraprocedural and postprocedural visualization of the exact position of the stent and the degree of stent deployment by using conventional radiographic techniques is suboptimal. Full stent deployment and good apposition of the stent margins to the arterial wall are of major importance in limiting subacute stent thrombosis. We present our preliminary experience in imaging of intracranial stents by using angiographic CT (ACT) with a new flat-detector angiographic system.

Technique and Cases

In three patients referred for intracranial stent placement, ACT was performed immediately after stent deployment. All patients were under general anesthesia. Using a flat-detector biplane angiographic system (Axiom Artis dBA; Siemens Medical Solutions, Erlangen, German), and with respiration suspended, we performed rotational radiography with new commercially available software (Dyna-CT). Parameters were as follows: 20 seconds, 0.4° increment, 512 matrix in projections, 220° total angle, 20°/second, approximately 15–30 frames/second, and 538 projections. Image postprocessing was performed to correct for scattered radiation, beam hardening, and ring artifacts on a workstation (Leonardo; Siemens Medical Solutions). Display of imaged stents was obtained by using multiplanar reconstructions (MPRs).

Received February 28, 2005; accepted after revision March 10.

From the Department of Radiology, Baylor College of Medicine (G.B., C.M.S., R.N., M.E.M.), the Department of Radiology, St. Luke's Hospital (H.M., M.E.M.), and the Department of Radiology, Methodist Hospital (G.B., G.M.S., R.K.), Houston, TX; and the Department of Cardio- and Vascular Surgery, Charité Humboldt University (B.C.), Berlin, Germany.

Address reprint requests to Götz Benndorf, MD, PhD, Department of Radiology, Baylor College of Medicine, Department of Radiology, One Baylor Plaza, 360, Houston, TX.

Case 1

A 66-year-old man was treated because of symptomatic 85% stenosis at the origin of the internal carotid artery (ICA). A long segment of irregular atherosclerotic plaque extended beyond the stenosis at the origin of the ICA. After a protective device (Accunet; Guidant Corporation, Menlo Park, CA) was placed in the distal cervical segment of the ICA, stent placement was done by using a 6–8 × 40-mm device (Acculink; Guidant Corporation). Because significant residual stenosis was present immediately after stenting, postdilation of the stent was performed by using a 6 × 30-mm balloon (Maverick, Boston Scientific, Natick, MA). This dilation resulted in less than 20% residual stenosis. ACT, three-dimensional (3D) digital subtraction angiography (DSA), and digital radiography were performed at the end of the procedure. Multiplanar reconstructions obtained with ACT showed extensive calcification in the carotid wall that compressed the segment of the stent that was not fully deployed. Axial views more clearly revealed the extent of calcification in the circumference of the arterial wall. Morphologic features of the plaque were not identifiable on DSA or digital radiography (nonsubtracted DSA images). This extensive wall calcification explained why the stent could not be fully deployed over its entire length (Fig 1).

Case 2

A 52-year-old man presented with recurrent right-arm weakness, numbness, and aphasia. MR imaging of the brain showed a minimal acute infarction in the posterior basal ganglia and corona radiata on the left, with minimal associated petechial hemorrhage. Cerebral angiography showed marked stenosis (80%) of the M1 segment of the left middle cerebral artery just beyond the origin of the anterior temporal artery Transcatheter placement of a 3 × 8-mm balloon-expandable stent (Cypher; Cordis, Miami Lakes, FL) into the left M1 segment was successfully performed, with restoration of normal flow and an excellent anatomic result. ACT, 3D DSA, and digital radiography were performed at the end of the procedure. The stent could hardly be identified on DSA and was only slightly more visible on nonsubtracted views. ACT allowed for complete visualization of the stent in every plane. The axial view demonstrated full and uniform deployment of the stent over its entire length. This finding could not be determined from the DSA or digital radiographic images (Fig 2).

Case 3

A 66-year-old man presented with multiple vertebrobasilar transient ischemic attacks due to a severe stenosis of the midbasilar artery, as shown on diagnostic angiography. 3D DSA showed a difference of approximately 0.5–1 mm in the diame-

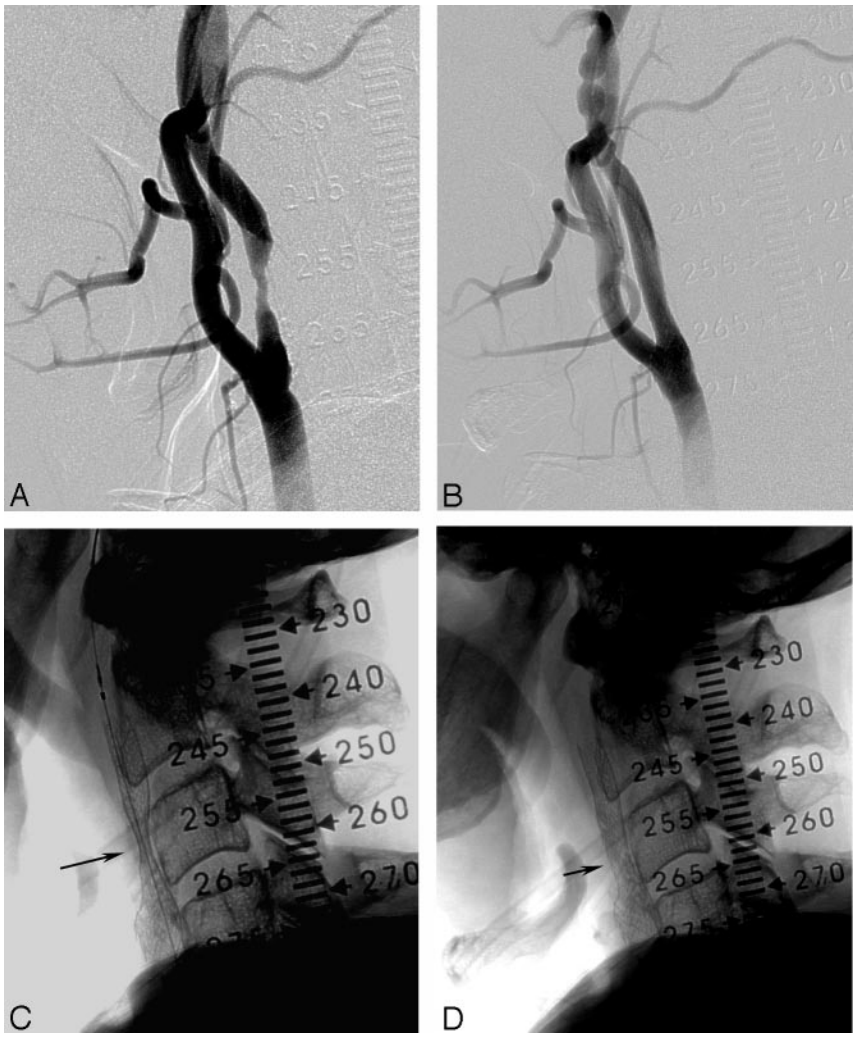

FIG 1. Stent placement in an extracranial carotid stenosis.

A, 85% stenosis of the ICA.

B, 6–8 × 40-mm stent (Acculink; Guidant Corporation) is placed.

C, Native image immediately after stenting shows a significant residual stenosis (*arrow*) requiring postdilation.

D, Satisfactory result and remaining minor narrowing (*arrow*). *(Fig 1 continues.)*

ters of the basilar artery above and below the stenosis. A 3 × 8-mm drug-eluting balloon-expandable stent (Cypher; Cordis) was successfully deployed across the stenotic segment. A postdeployment angiogram demonstrated apparently good apposition of the stent to the arterial wall, with restoration of the internal luminal diameter and good anterograde flow. However, angiography showed significant differences in the diameters of the distal and proximal segments of the basilar artery into which the stent was anchored. Therefore, the balloon was advanced into the distal portion of the stent, where it was inflated to overexpand this segment. No evidence of dissection, platelet aggregation, or branch occlusion was observed. The patient awoke from general anesthesia, and results of his baseline neurologic examination were normal (Fig 3).

Discussion

The design requirements of stents suitable for use in the intracranial circulation (eg, low profile, high flexibility, trackability, adequate radial strength) have thus far substantially limited the ability to construct devices with sufficient radiopacity for adequate angiographic visualization. This limitation, combined with the ability to only indirectly visualize the arterial wall of intracranial vessels, has made it difficult (if not impossible) to be certain regarding the exact position or full deployment of a stent and its apposition to the arterial wall. Although experience in intracranial stent placement for stent-assisted coiling of aneurysms and for atherosclerotic lesions is still limited, our personal experience and reports from the cardiology literature indicate that good visualization of the position, orientation, and degree of deployment of the stent is important in obtaining good outcomes (1). As stents are increasingly used to treat atherosclerotic disease and as novel stent-placement protocols (placement of double stents, covered stents, and stents with variable strut densities) are used to treat aneurysms, the need for their clear visualization will increase. Therefore, the radiopacity of stents is an important feature (2, 3), especially with intracranial applications in which stents are small, short, and superimposed on the bony structures of the skull. Cases 2 and 3 seem to indicate that the availability of ACT in the angiographic suite considerably improves visualization of these devices.

The spatial resolution of our flat-panel detector system was about 200 μm (detector element = 154 μm). Although the struts of some intracranial stents (eg, 141 μm for Cypher; Cordis) are smaller than this,

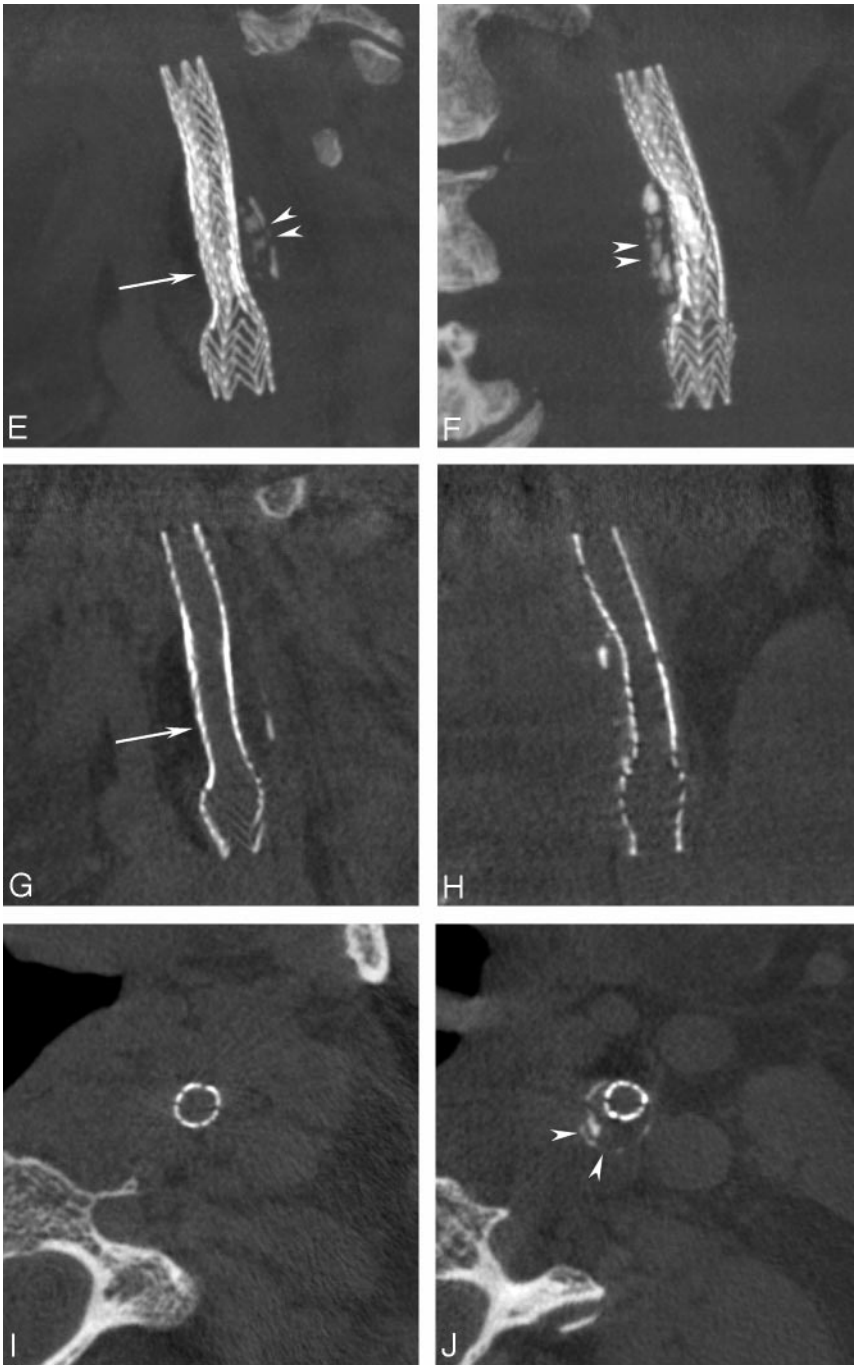

FIG 1. *Continued.*

E and *F* MPRs, Lateral (*E*) and coronal (*F*) ACT views (5-mm sections) provide superior visualization of the entire stent, its struts, and the remaining narrowing (*arrow*) and show the underlying, heavily calcified plaque (*arrowheads*) responsible for incomplete stent deployment.

G and *H*, Reducing the section thickness to 0.1 mm allows visualization along a cut plane through the center of the stent, showing the effective remaining narrowing (arrow).

I and *J*, On axial views, the different diameters of the recanalized lumen distal to and at the level of the plaque are appreciated. They further reveal the circumferential narrowing by the calcified plaque (*arrowheads* in *J*). Note visualization of soft-tissue components in the neck.

they may still be visualized on reconstructed images made from the volume acquisition. In this sense, ACT works like a magnifying glass, depicting structures that are smaller than the technical spatial resolution of the detector system used for the acquisition.

Duplex sonography and CT angiography play an important role in the preoperative and postoperative assessment of stented or operated extracranial carotid stenosis (4, 5). Duplex sonography has been proven useful (6) for the preoperative characterization of plaque morphology; however, it is relatively operator-dependent. For follow-up of intracranial stenoses, CT angiography can be used to assess vascular patency after stents are placed in small vessels, such intracranial arteries (7). However, in vitro studies have demonstrated that the degree of in-stent stenosis tends to be overestimated (8). For immediate postprocedural CT angiography, the patient must be transported. However, mobilization and transportation to a CT scanner can cause a substantial loss of time and compromise monitoring and care of the patient during the transfer. Rapidly performing ACT while the patient remains on the angiographic table may be a feasible option.

As shown in case 1, ACT may also be used for some degree of tissue characterization before stent

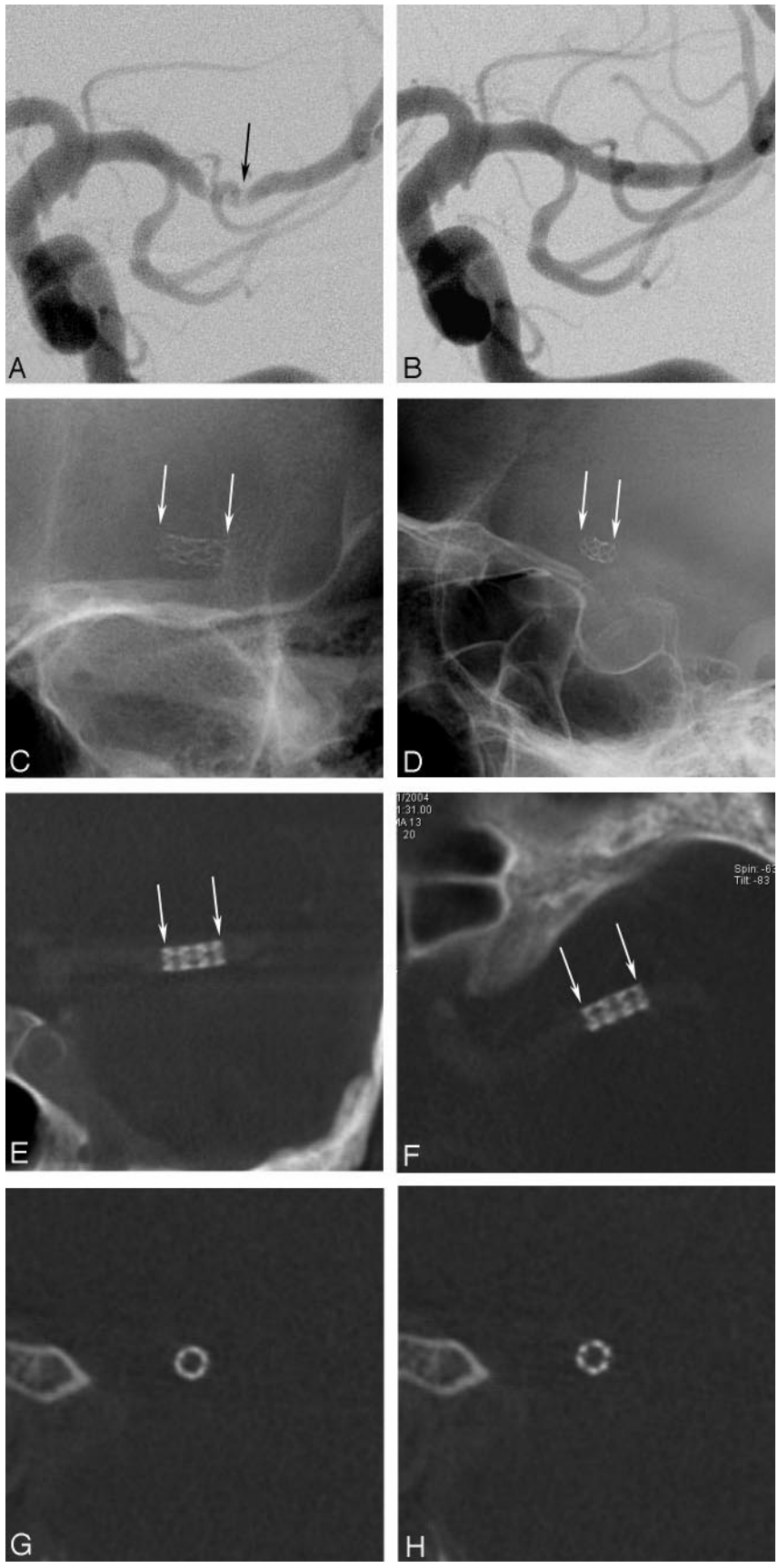

FIG 2. Stent placement in an 80% stenosis of the intracranial middle cerebral artery.

A, High-grade stenosis (*arrow*) of the left M1 segment

B, Treatment with a 3 × 8-mm drug-eluting stent (Cypher; Cordis) was successful, completely reestablishing the lumen.

C and *D*, Nonsubtracted images permit moderate visualization of the deployed stent (*arrows*).

E and *F*, Coronal and axial MPRs allow superior visualization of the stent (*arrows*).

G and *H*, Orthogonal views ("down the barrel") through the inner lumen of the stent at its proximal and distal ends show complete and symmetric deployment.

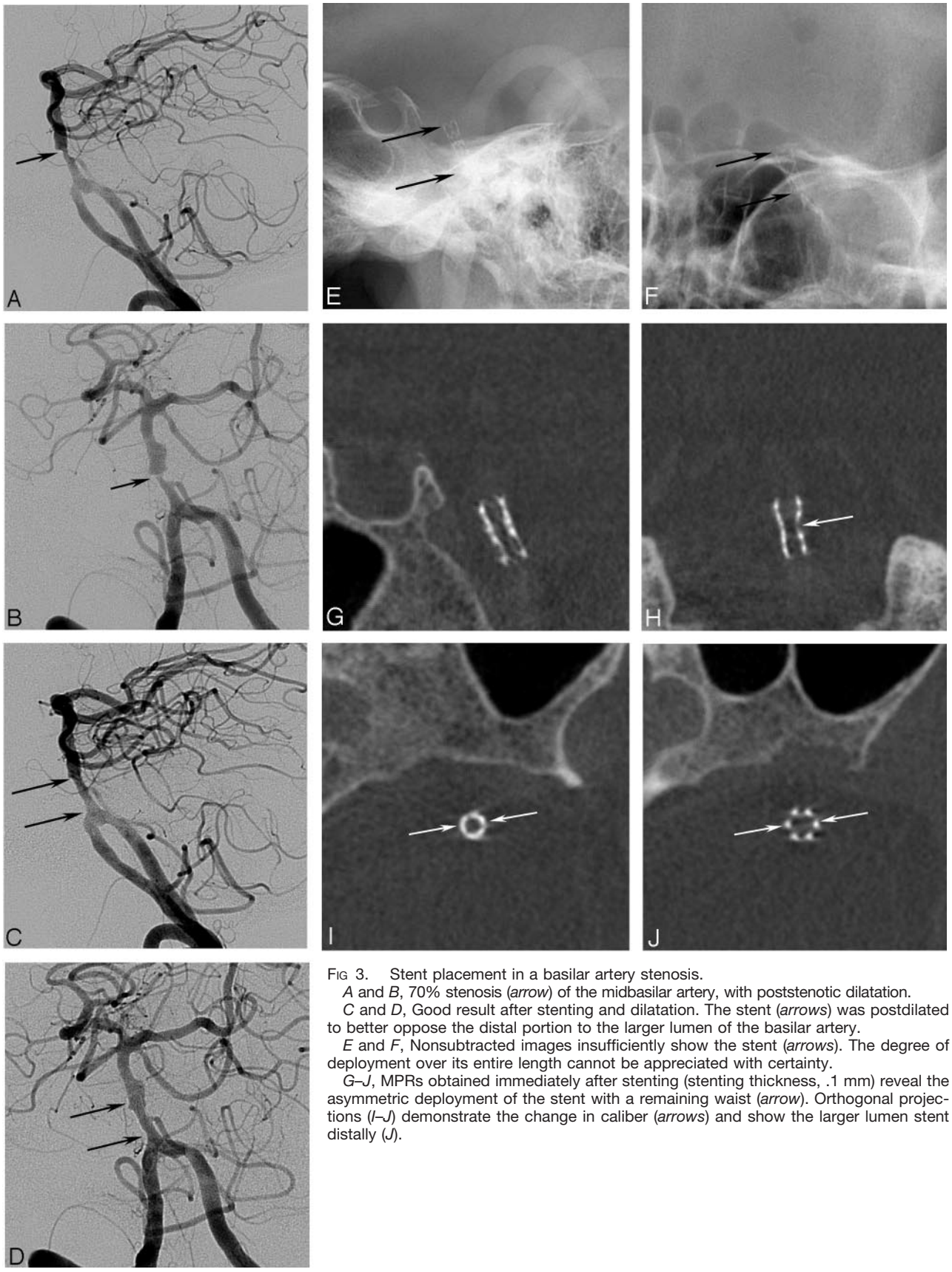

FIG 3. Stent placement in a basilar artery stenosis.

A and *B*, 70% stenosis (*arrow*) of the midbasilar artery, with poststenotic dilatation.

C and *D*, Good result after stenting and dilatation. The stent (*arrows*) was postdilated to better oppose the distal portion to the larger lumen of the basilar artery.

E and *F*, Nonsubtracted images insufficiently show the stent (*arrows*). The degree of deployment over its entire length cannot be appreciated with certainty.

G–J, MPRs obtained immediately after stenting (stenting thickness, .1 mm) reveal the asymmetric deployment of the stent with a remaining waist (*arrow*). Orthogonal projections (*I–J*) demonstrate the change in caliber (*arrows*) and show the larger lumen stent distally (*J*).

placement, as well as for immediate procedural monitoring and poststenting control. It may offer valuable, detailed information while a patient is still on the angiographic table, and thus, it may aid in clinical decision making.

References

1. Honda Y, Fitzgerald PJ. **Stent thrombosis: an issue revisited in a changing world.** *Circulation* 2003;108:2–5
2. Fischell TA. **Visible stents: all that glitters. Is it gold?** *J Invasive Cardiol* 2000;12:233–235
3. Wiskirchen J, Kraemer K, Konig C, et al. **Radiopacity of current endovascular stents: evaluation in a multiple reader phantom study.** *J Vasc Interv Radiol* 2004;15:843–852
4. Prokop M, Waaijer A, Kreuzer S. **CT angiography of the carotid arteries.** *JBR BTR* 2004;87:23–29
5. Schuknecht B. **Latest techniques in head and neck CT angiography.** *Neuroradiology* 2004;46:s208–213
6. AbuRahma AF, Covelli MA, Robinson PA, Holt SM. **The role of carotid duplex ultrasound in evaluating plaque morphology: potential use in selecting patients for carotid stenting.** *J Endovasc Surg* 1999;6: 59–65
7. Hahnel S, Trossbach M, Braun C, et al. **Small-vessel stents for intracranial angioplasty: in vitro comparison of different stent designs and sizes by using CT angiography.** *AJNR Am J Neuroradiol* 2003;24:1512–1516
8. Trossbach M, Hartmann M, Braun C, Sartor K, Hahnel S. **Small vessel stents for intracranial angioplasty: in vitro evaluation of in-stent stenoses using CT angiography.** *Neuroradiology* 2004;46: 459–463